

Metal-Organic Framework Derived NiS₂ Hollow Spheres as Multifunctional Reactors for Synergistic Regulation of Polysulfides Confinement and Redox Conversion

Shunyou Hu^{a+}, Mingjie Yi^{a+}, Sajid Hussain Siyal^c, Dong Wu^a, Hao Wang^a, Zhenye Zhu^{a, *}, Jiaheng Zhang^{a, b *}

^aResearch Centre of Printed Flexible Electronics, School of Materials Science and Engineering, Harbin Institute of Technology, Shenzhen 518055, China.

^bState Key Laboratory of Advanced Welding and Joining, Harbin Institute of Technology, Shenzhen 518055, China.

^cDepartment of Metallurgy and Materials Engineering, Dawood University of Engineering and Technology, Karachi 74800, Sindh, Pakistan.

⁺These authors contributed equally to this work.

Corresponding author:

Jiaheng Zhang, Email: zhangjiaheng@hit.edu.cn

Zhenye Zhu, Email: zhuzy@hit.edu.cn

Experimental section

1. The preparation process of C HSs

In a typical procedure, after carbonization of Ni-MOF under 450 °C for 6 h, the obtained Ni/C HSs powder was etched in 2 M HCl aqueous solution under 150 °C for 24 h. After cooling to room temperature, the C HSs powder was collected and washed with deionized water and ethanol for 3 times, respectively.

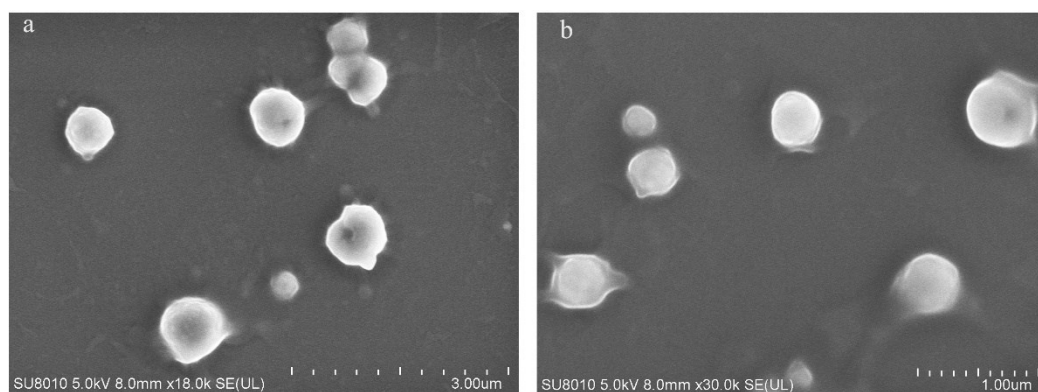


Fig. S1 SEM images of Ni-MOF.

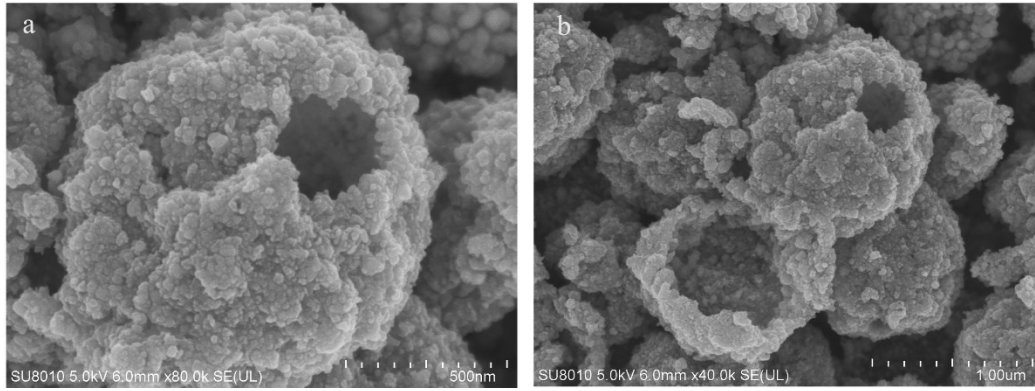


Fig. S2 SEM images of NiS₂/C HSs.

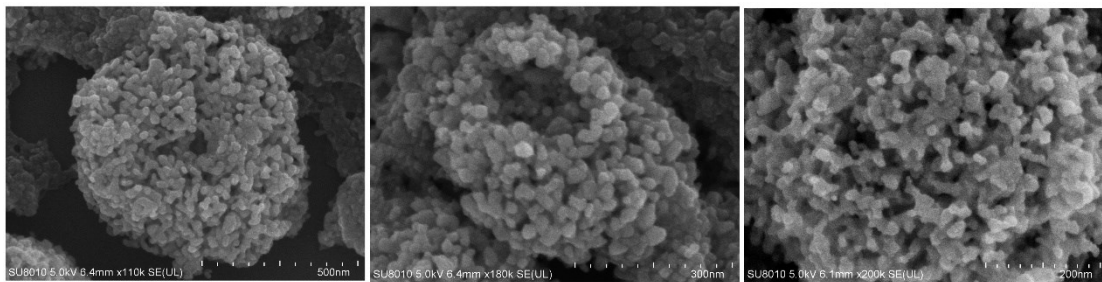


Fig. S3 SEM images of C HSs.

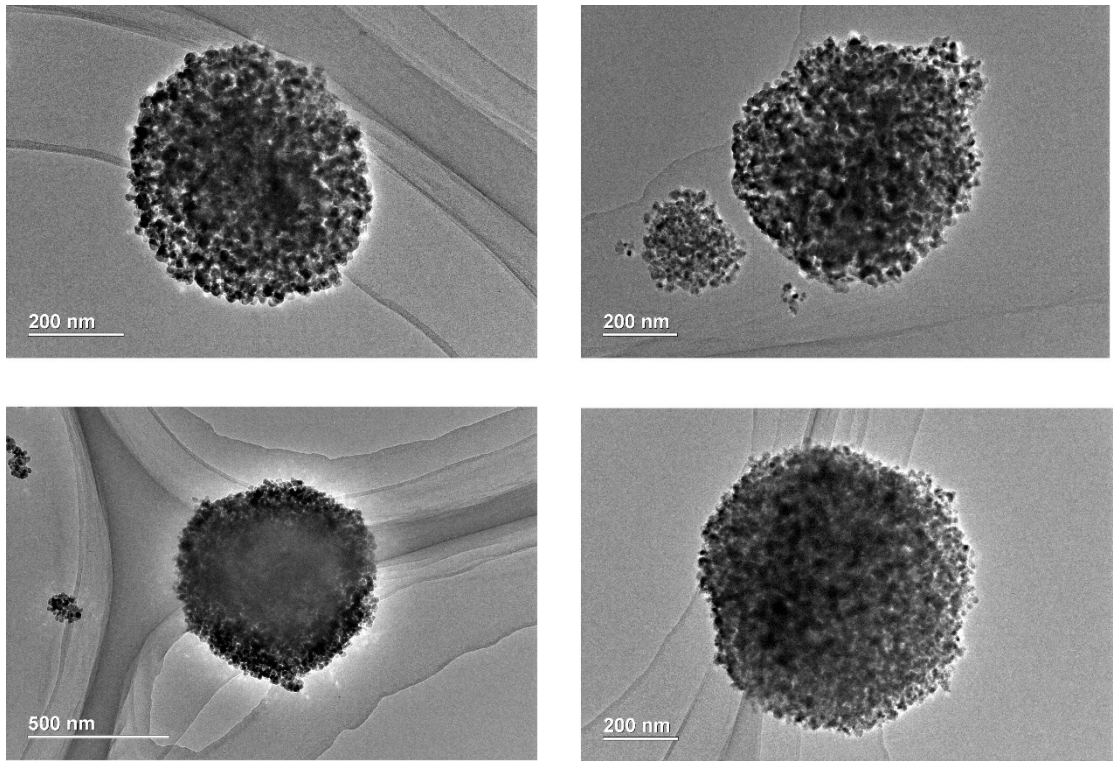


Fig. S4 TEM images of NiS₂/C HSs.

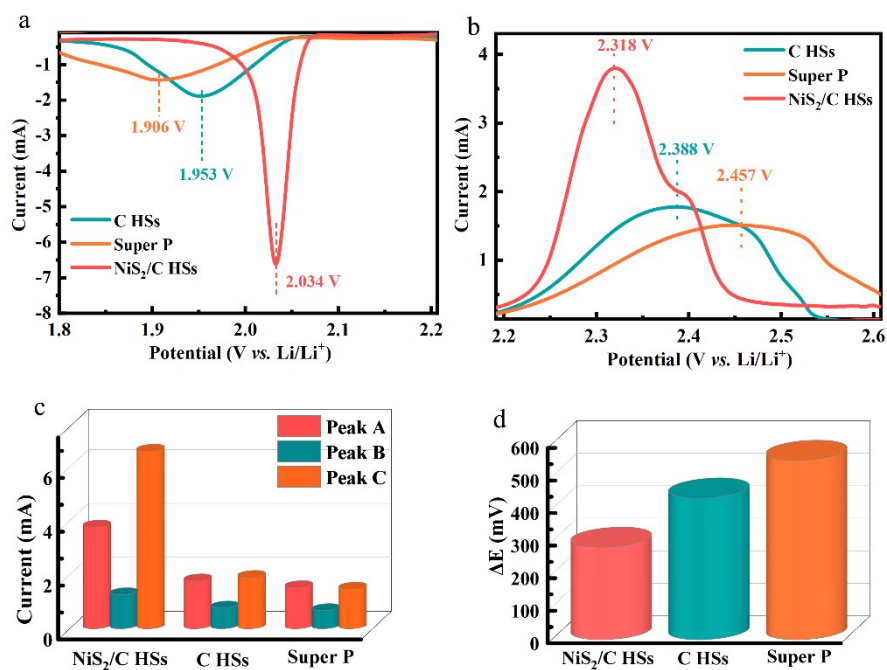


Fig. S5 The enlarged CV profiles of peak C (a) and peak A (b) of Li-S batteries with different cathodes. The current of the peak A, peak B and peak C of the CV profiles (c). The potential difference between peak A and peak C (d).

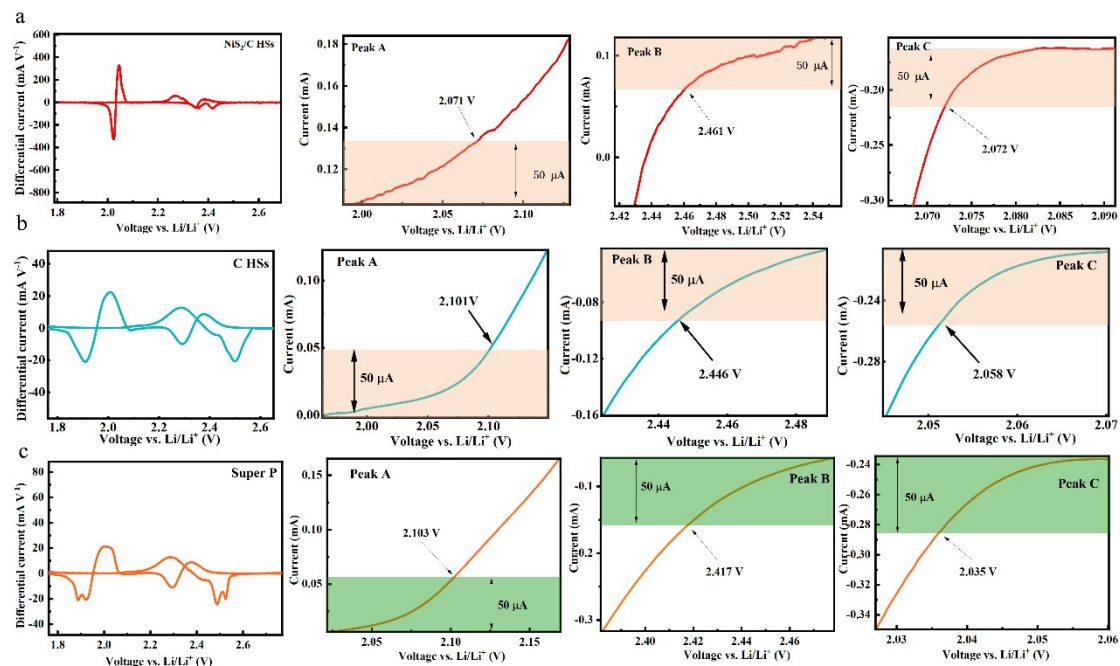


Fig. S6 Onset potential measurement of Li-S batteries with NiS₂/C HSs (a), C HSs (b) and Super P (c). The baseline current are obtained from the values before the cathodic and anodic peaks, where the value of current remain almost unchanged and the value of $dI/dV \approx 0$ ². The onset current is 50 μ A beyond the baseline current (50 μ A more negative than baseline current for cathodic peak and 50 μ A more positive than baseline current for anodic peak)².

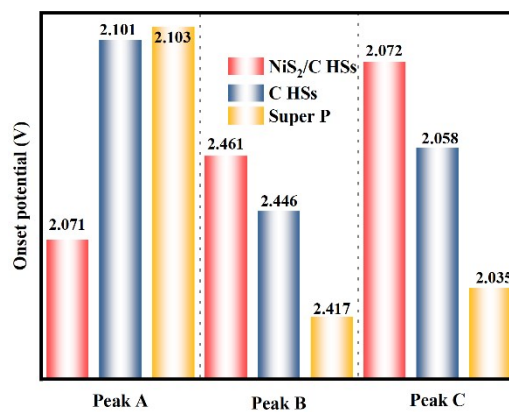


Fig. S7 The onset potential of Li-S batteries with NiS₂/C HSs, C HSs and Super P.

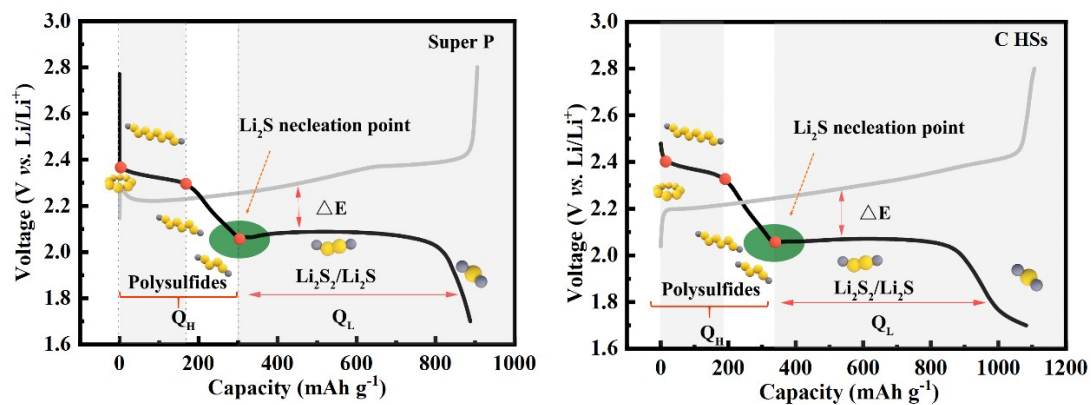


Fig. S8 The charge/discharge profiles of the cells with Super P and C HSs.

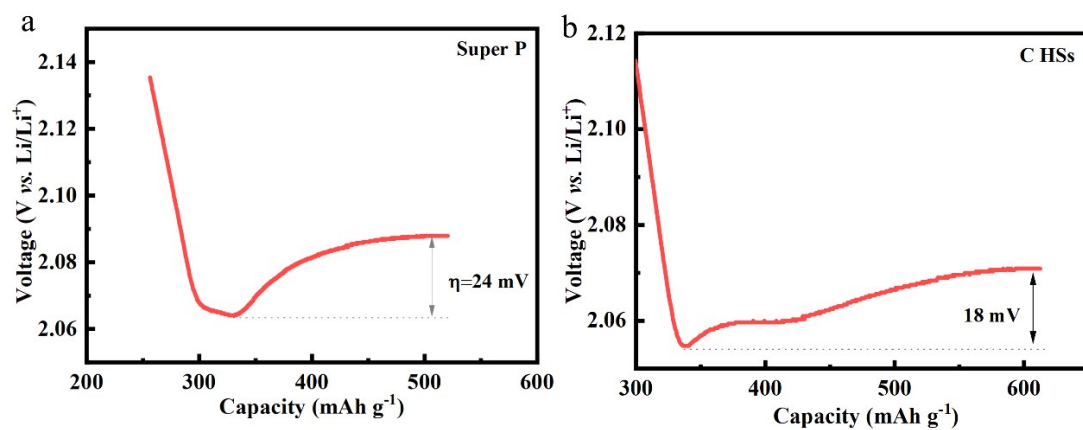


Fig. S9 The nucleation overpotential of Li_2S of the cells with Super P (a) and C HSs (b).

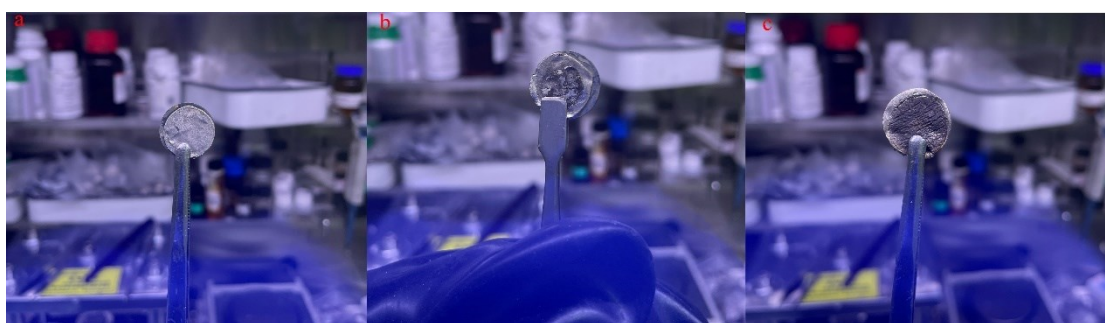


Fig. S10 The digital photographs of Li anode disassembled from the Li-S cells with NiS_2/C HSs (a), C HSs (b) and Super P (c).

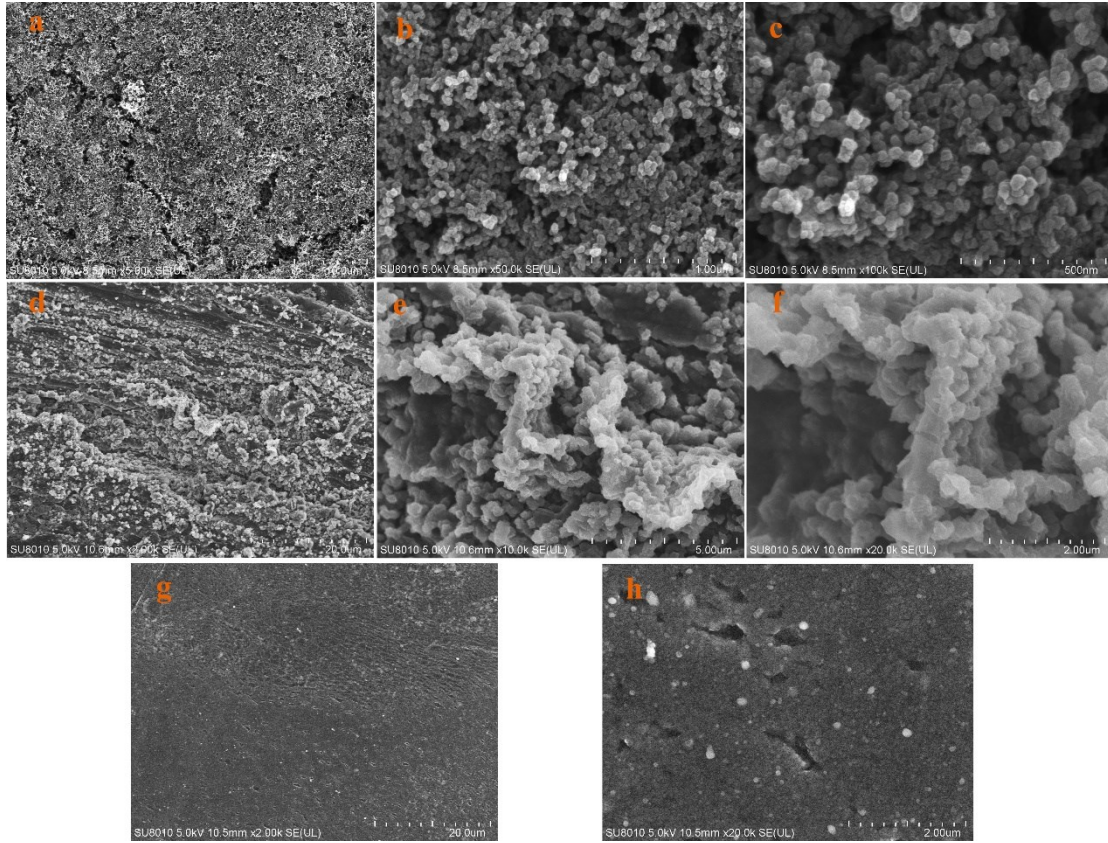


Fig. S11 SEM images of Li anode of the cells with C HSs (a-c), Super P (d-f), and NiS₂/C HSs (g, h).

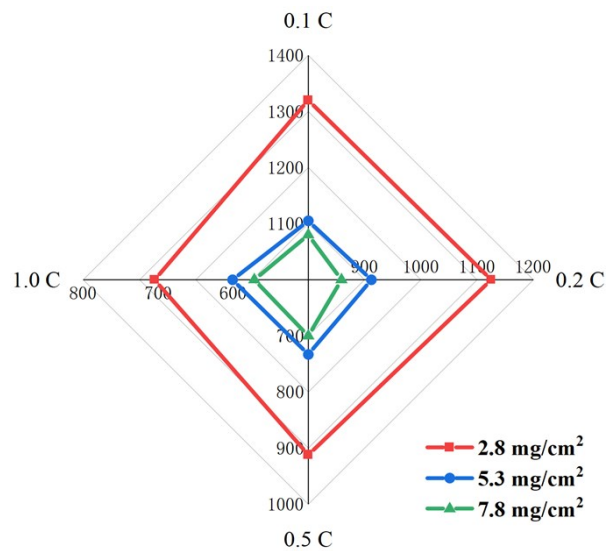


Fig. S12 The rate performance of the cells with NiS₂/C HSs under 2.8 mg/cm², 5.3 mg/cm² and 7.8 mg/cm² sulfur loadings.

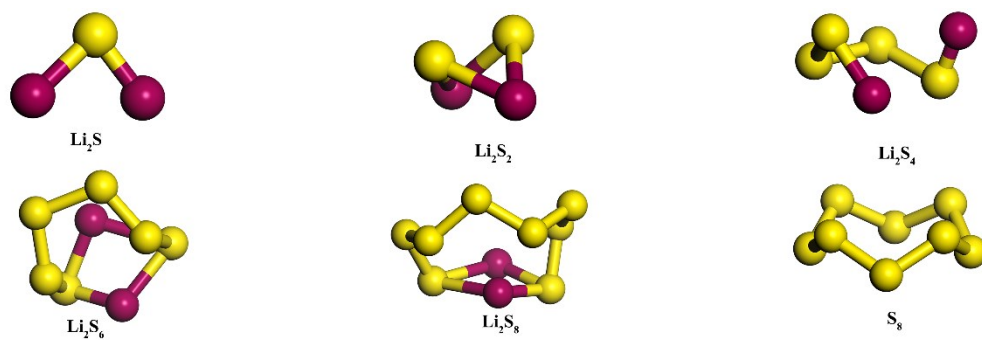


Fig. S13 The optimized geometries of Li_2S , Li_2S_2 , Li_2S_4 , Li_2S_6 , Li_2S_8 and S_8 .

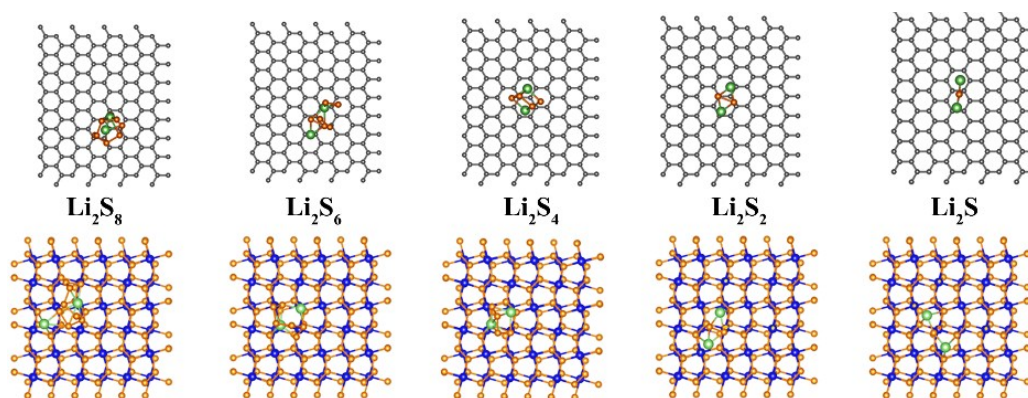


Fig. S14 Optimized configurations of polysulfides adsorption on graphene and NiS_2 .

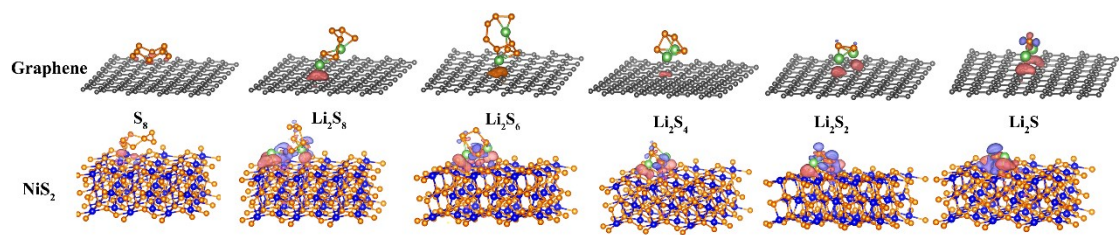


Fig. S15 The charge density difference of polysulfides adsorbed at graphene and NiS_2 , in which, blue denoted the decrease of charge and red denoted charge accumulation.

Table. S1 The electrochemical performance of various cathodes of Li-S batteries.

Cathode	Current rate (C)	Area loading (mg cm ⁻²)	Areal capacity (mAh cm ⁻²)	Ref.
NiS ₂ /C HSs	0.2	7.8	6.6	This work
NiS ₂ /C HSs	0.2	5.3	4.8	This work
NiS ₂ /C HSs	0.2	2.8	3.1	This work
Co,N-G@CNT/S	0.2	4.2	4.4	3
S@CPZC	0.2	9.2	7.1	4
S@CPZC	0.2	5.1	4.7	4
H-S@Co-CNCs	0.2	4.0	2.7	5
CNT-NC@GC/S	0.2	3.36	3	6
S@H-LDH	0.2	1.5	1.3	7
CNF/LPS/CNT	0.2	7.64	3.5	8
S/CoNi@PNCFs	0.2	4.5	4	9
Sb ₂ Se _{3-x} /rGO	0.2	3	2.9	10
NC/MoS ₃ -S NBs	0.2	5.5	4.5	11
COF-MF@S	3.43 mA cm ⁻²	4.1	3.7	12
N-PC@uCo/S	0.2	5.9	4.8	13
3WO ₃ -WS ₂ /S	0.5	5.0	4.4	14
3WO ₃ -WS ₂ /S	0.5	10.0	4.7	14
ZnS _{1-x} -CC/S	0.1	5.0	3.5	15
NiCoO ₄ /CNF/S	0.1	6.9	4.6	16

References

- 1 J. Li, J. Li, D. Yan, S. Hou, X. Xu, T. Lu, Y. Yao, W. Mai and L. Pan, *J. Mater. Chem. A*, 2018, **6**, 6595-6605.
- 2 W. Yao, W. Zheng, J. Xu, C. Tian, K. Han, W. Sun and S. Xiao, *ACS Nano*, 2021, DOI: 10.1021/acsnano.1c00270.
- 3 D. Cheng, Y. Zhao, X. Tang, T. An, X. Wang, H. Zhou, D. Zhang and T. Fan, *Carbon*, 2019, **149**, 750-759.
- 4 G. Li, W. Lei, D. Luo, Y. Deng, Z. Deng, D. Wang, A. Yu and Z. Chen, *Energy Environ. Sci.*, 2018, **11**, 2372-2381.
- 5 Q. Wu, X. Zhou, J. Xu, F. Cao and C. Li, *ACS Nano*, 2019, **13**, 9520-9532.
- 6 F. Zhou, Z. Qiao, Y. Zhang, W. Xu, H. Zheng, Q. Xie, Q. Luo, L. Wang, B. Qu and D.-L. Peng, *Electrochim. Acta*, 2020, **349**, 136378.
- 7 S. Chen, J. Luo, N. Li, X. Han, J. Wang, Q. Deng, Z. Zeng and S. Deng, *Energy Storage Mater.*, 2020, **30**, 187-195.
- 8 Y. Li, C. Wang, W. Wang, A. Y. S. Eng, M. Wan, L. Fu, E. Mao, G. Li, J. Tang, Z. W. Seh and Y. Sun, *ACS Nano*, 2020, **14**, 1148-1157.
- 9 Y. He, M. Li, Y. Zhang, Z. Shan, Y. Zhao, J. Li, G. Liu, C. Liang, Z. Bakenov and Q. Li, *Adv Funct Mater*, 2020, **30**, 2000613.
- 10 Y. Tian, G. Li, Y. Zhang, D. Luo, X. Wang, Y. Zhao, H. Liu, P. Ji, X. Du, J. Li and Z. Chen, *Adv. Mater.*, 2020, **32**, 1904876.
- 11 J. Yu, J. Xiao, A. Li, Z. Yang, L. Zeng, Q. Zhang, Y. Zhu and L. Guo, *Angew. Chem.-Int. Edit.*, 2020, **59**, 13071-13078.
- 12 X. Hu, J. Jian, Z. Fang, L. Zhong, Z. Yuan, M. Yang, S. Ren, Q. Zhang, X. Chen and D. Yu, *Energy Storage Mater.*, 2019, **22**, 40-47.
- 13 R. Wang, J. Yang, X. Chen, Y. Zhao, W. Zhao, G. Qian, S. Li, Y. Xiao, H. Chen, Y. Ye, G. Zhou and F. Pan, *Adv. Energy Mater.*, 2020, **10**, 1903550.
- 14 B. Zhang, C. Luo, Y. Deng, Z. Huang, G. Zhou, W. Lv, Y.-B. He, Y. Wan, F. Kang and Q.-H. Yang, *Adv. Energy Mater.*, 2020, **10**, 2000091.
- 15 J. Wang, Y. Zhao, G. Li, D. Luo, J. Liu, Y. Zhang, X. Wang, L. Shui and Z. Chen, *Nano Energy*, 2021, **84**, 105891.
- 16 J.-X. Lin, X.-M. Qu, X.-H. Wu, J. Peng, S.-Y. Zhou, J.-T. Li, Y. Zhou, Y.-X. Mo, M.-J. Ding, L. Huang and S.-G. Sun, *ACS Sustain. Chem. Eng.*, 2021, **9**, 1804-1813.